

Lawrence Berkeley National Laboratory

Recent Work

Title

A MICROSTRUCTURAL STUDY OF THE THERMAL FATIGUE FAILURES OF 60Sn-40 Pb SOLDER JOINTS

Permalink

<https://escholarship.org/uc/item/2471d66g>

Author

Morris, J.W.

Publication Date

1987-12-01

Center for Advanced Materials

CAM

RECEIVED
LAWRENCE
BERKELEY LABORATORY

MAR 4 1988

Submitted to Journal of Electronic Materials

LIBRARY AND
DOCUMENTS SECTION

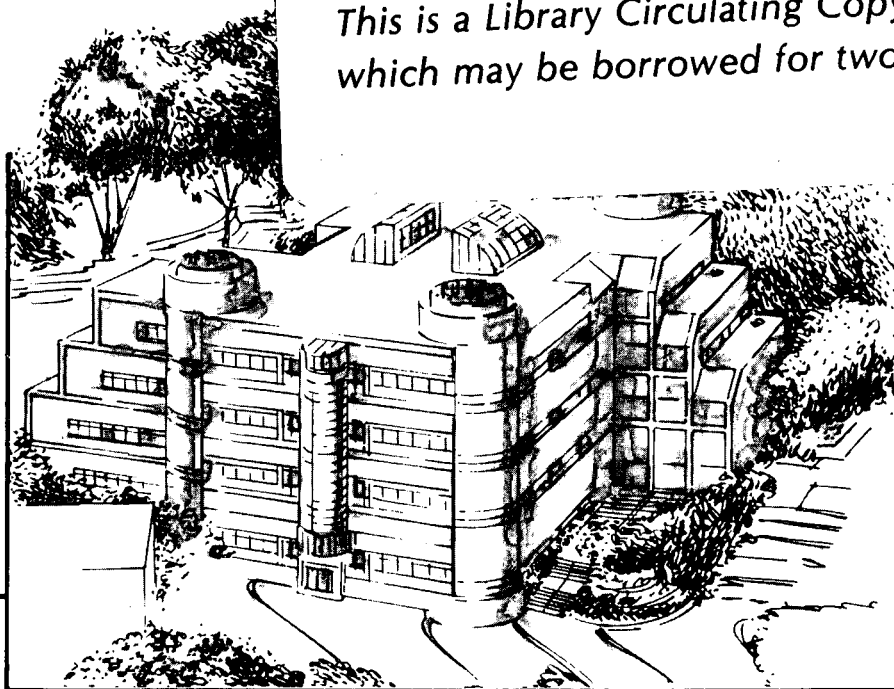
A Microstructural Study of the Thermal Fatigue Failures of 60Sn-40 Pb Solder Joints

D. Frear, D. Grivas, and J.W. Morris, Jr.

December 1987

TWO-WEEK LOAN COPY

*This is a Library Circulating Copy
which may be borrowed for two weeks.*



Materials and Chemical Sciences Division

Lawrence Berkeley Laboratory • University of California

ONE CYCLOTRON ROAD, BERKELEY, CA 94720 • (415) 486-4755

LBL-24488
c.2

DISCLAIMER

This document was prepared as an account of work sponsored by the United States Government. While this document is believed to contain correct information, neither the United States Government nor any agency thereof, nor the Regents of the University of California, nor any of their employees, makes any warranty, express or implied, or assumes any legal responsibility for the accuracy, completeness, or usefulness of any information, apparatus, product, or process disclosed, or represents that its use would not infringe privately owned rights. Reference herein to any specific commercial product, process, or service by its trade name, trademark, manufacturer, or otherwise, does not necessarily constitute or imply its endorsement, recommendation, or favoring by the United States Government or any agency thereof, or the Regents of the University of California. The views and opinions of authors expressed herein do not necessarily state or reflect those of the United States Government or any agency thereof or the Regents of the University of California.

**A MICROSTRUCTURAL STUDY OF THE
THERMAL FATIGUE FAILURES OF
60SN-40 PB SOLDER JOINTS**

D. FREAR*, D. GRIVAS, J. W. MORRIS, JR.****

**Center for Advanced Materials
Materials and Chemical Sciences Division
Lawrence Berkeley Laboratory
University of California**

and

**Department of Materials Science and Mineral Engineering
University of California at Berkeley
Berkeley, California 94720**

December 1987

**This work is supported by the Director, Office of Energy Research,
Office of Basic Energy Science, Materials Sciences Division of the
U. S. Department of Energy under Control No. DE-AC03-76SF00098**

A MICROSTRUCTURAL STUDY OF THE THERMAL FATIGUE FAILURES OF 60SN-40PB SOLDER JOINTS.

D. FREAR*, D. GRIVAS**, J. W. MORRIS, JR.**

* Currently at:
Sandia National Laboratory
Division 1832
P. O. BOX 5800
Albuquerque, NM 87185

** Center for Advanced Materials
Lawrence Berkeley Laboratory and
Department of Materials Science
University of California, Berkeley
Berkeley, CA 94720

ABSTRACT

When an electronic package encounters thermal fluctuations, cyclical shear strain is imposed on the solder joint interconnections. The thermal cycling leads to a condition of thermal fatigue and eventual solder joint failure. This study was performed in order to understand the microstructural mechanisms that lead to solder joint failures in thermal fatigue. Thermal cycling tests were performed on 60Sn-40Pb joints using a -55°C to 125°C cycle and 19% imposed shear strain. A heterogeneously coarsened region of both Pb and Sn-rich phases develops within the 60Sn-40Pb solder joints. Cracks initiate in the heterogeneously coarsened Sn-rich phase at the Sn-Sn grain boundaries. Heterogeneous coarsening and failure occurs in both high (35°C to 125°C) and low (-55°C to 35°C) thermal cycles. The elevated temperature portion of the thermal cycle was found to be the most significant factor in the heterogeneous coarsening and failure of the solder joints.

Key Words: Sn-Pb Solder, Microstructure, Low Cycle Thermal Fatigue.

INTRODUCTION

Thermal fatigue failures of solder joints in electronic packages is of critical concern in the microelectronics industry. The cause of these failures is a combination of thermal fluctuations experienced by the package and the materials of differing thermal expansion coefficients used in the package. When an electronic package encounters thermal fluctuations cyclical strain is imposed upon the solder joints which eventually leads to joint failure. The source of fluctuations that result in thermal fatigue can be either environmental (variations due to thermal variations in the ambient environment) or due to power cycling (thermal variations caused by heat dissipation of the device within the package). The failure of solder joints of electronic components due to thermal fatigue is well documented¹⁻¹⁵. To further complicate the thermal fatigue problem the trend in microelectronic packaging is towards larger integrated chips (and therefore larger chip carriers) surface mounted on circuit boards. As carriers become larger the strains imposed upon solder joints also increases thereby exacerbating failures in thermal fatigue. Therefore the thermal fatigue behavior of solder joints must be better understood to alleviate the problem of thermal fatigue. A microstructural analysis of solder joints in thermal fatigue is the most appropriate method to perform this study.

The solder joints in an electronic package encounter a complicated state of strain in thermal cycling, although the primary strain state is in shear¹⁶. This would make a fundamental study of the microstructural evolution in thermal fatigue difficult to interpret on actual joints in an electronic package. Therefore for the work in this study a simplified solder joint was designed that experiences simple shear on thermal cycling^{17,18}.

Previous studies on Sn-Pb solder joints show that a clear understanding of how solder joint microstructure influences thermal fatigue behavior is lacking. Conclusions as to the cause of thermal fatigue failures range from failure through interfacial intermetallics^{2,19-23} to bulk solder failures^{3,5,7,12,24,25}. From these varied positions it is impossible to state conclusively what the cause of thermal fatigue failures is, and furthermore, how to

eliminate or delay failures. Therefore the purpose of this study is to document, and understand, the microstructural development of 60Sn-40Pb solder joints in thermal fatigue in a shear configuration. These observations make it possible to characterize the microstructural causes of failures in thermal fatigue.

EXPERIMENTAL PROCEDURE

To perform thermal fatigue tests a specimen was designed that would impose strains on a solder joint under thermal cycling conditions. This design is shown in Figure 1. The design consists of an aluminum plate sandwiched between two copper plates. The aluminum was plated with 0.05 mm (0.002 in) of Ni to act as a diffusion barrier, and a 0.025 mm (0.001 in) of Cu to give the solder joint a similar interface on each side. The specimens were manufactured as described in a previous paper¹⁸. The Al has a thermal expansion coefficient of $25 \mu\text{in/in}^\circ\text{C}$ while that of Cu is $16.6 \mu\text{in/in}^\circ\text{C}$ so upon thermal cycling a maximum strain is imposed upon the ends of the specimen and decreases linearly to zero in the center. The magnitude of strain imposed is increased by either lengthening the specimen or by decreasing the solder joint thickness. For the experiments in this study a maximum 19% shear strain was imposed on the joints at the ends of the specimen.

Thermal cycling was performed using the apparatus shown schematically in Figure 2. The device consists of a digitally controlled crane that automatically cycles specimens between two thermal baths. The high temperature bath consists of resistively heated oil with an accuracy of $\pm 1^\circ\text{C}$. The low temperature bath was made using ethyl alcohol cooled by a liquid nitrogen through a Cu coil with an accuracy of $\pm 5^\circ\text{C}$. The low temperature was controlled by varying the liquid nitrogen flow rate. The use of liquid baths had a two fold purpose. First, using a liquid medium reduces the oxidation specimens would receive in air, and thus eliminates a complication to the results. Secondly, the liquid gives a rapid heat transfer which allows for an accelerated fatigue test.

The hold time in each bath was 5 minutes with a transfer time of 30 seconds. Microstructural evolution versus the number of thermal cycles was evaluated by placing a number of specimens in the cycling device and removing individual specimens after a number of cycles.

Specimens for optical microstructural observations were successively ground down to 600 grit silicon carbide paper under flood cooling. The samples were then polished on felt paper using an Al_2O_3 /kerosene mixture. Final polishing and etching were performed simultaneously using a colloidal slurry of $0.03\ \mu\text{m}$ silicon carbide particles in a slightly acidic solution. Special care was necessary in the polishing of these specimens because the Cu and Al became galvanically coupled causing the Al to severely pit and interfere with the joint interface. This problem was solved by polishing the specimen for only short times (on the order of 5 minutes) in the colloidal solution. This technique clearly revealed the solder microstructure.

Bulk 60Sn-40Pb solder specimens for TEM observation were punched into 3 mm disks and hand polished to a 2 mil thickness. Electropolishing was performed using 85% ethyl alcohol + 5% 2-butoxyethynol + 10% perchloric acid at 30-34 volts and 80 mA current. Immediately before polishing both sides of the foil were ground with 600 grit paper to remove surface oxide. After electropolishing the foils were cold stage ion milled for 10 minutes at 5 KeV and 0.3 mA/gun at a tilt of 13° . TEM observations were made using the Kratos HVEM operated at 1.5 MeV.

RESULTS

-55 °C to 125 °C Thermal Cycle

Thermal fatigue specimens, shown in Figure 1 with 10 mil (0.254 mm) thick 60Sn-40Pb joints, were thermally cycled between -55°C and 125°C up to 2000 cycles. The optical microstructure of these joints as a function of number of cycles is shown in Figure 3. An interesting development in the microstructural evolution was found to occur after

625 cycles, the microstructure in the bulk solder heterogeneously coarsens parallel to the direction of shear in the regions of high shear strain at the ends of the specimen. This is shown clearly in Figure 4 which is a specimen after 684 thermal cycles. Both the Pb and Sn-rich phases coarsen. The coarsened Pb-rich phase is devoid of Sn precipitates. The coarsening is not associated with the Cu/solder interface, heterogeneous coarsened regions occur anywhere from near the interface to the center of the joint. The coarsened regions show no preference to form either on the Cu or Al side of the joint. The coarsened regions initially are very thin but gradually increase in width as the number of cycles increases.

After 1000 cycles cracks develop in the heterogeneous coarsened region of the solder, Figure 3. These cracks are found to occur only within the heterogeneously coarsened regions of the solder joint, as shown in Figure 5. The crack follows the coarsened region as it tails down from right to left across the joint. The cracks occur through the Sn-rich regions or at the interface between the Sn-rich and Pb-rich regions. This is clearly shown in the polarized optical micrographs in Figure 6 of the specimen after 1300 cycles. The cracks occur through the Sn-rich regions at Sn-Sn grain boundaries. In polarized light different Sn grains show variations in contrast and cracks are observed between these variations in contrast. The cracks propagate through Pb-rich regions so as to join failed Sn-rich regions. The Sn grains observed in the polarized micrographs are about 3 μm in diameter. The Sn grain size of the as-solidified solder is 0.44 μm , shown in the TEM micrographs of Figure 7. The Sn grain size for bulk solder aged at 125°C for 167 hours (which is equivalent to 2000 cycles with a 5 minute hold time) coarsened to 1.3 μm , as shown in the TEM micrograph of Figure 8. The Sn grains in the highly strained coarsened regions therefore grow larger than expected for thermal aging alone.

To determine the effect of joint thickness 60Sn-40Pb solder joint specimens of 20 mil (0.51 mm) thickness were also thermally cycled between -55°C and 125°C. By doubling joint thickness the shear strain was halved to 10%. The results of this experiment are

shown in Figure 9. Again heterogeneous coarsened regions develop throughout the solder. After 1000 cycles multiple coarsened regions occur parallel to the shear direction. More than one heterogeneous region was observed in each sample. Despite the halved strain the joints fail, through the coarsened region, after 1000 cycles. This is the same as for the 19% shear strained samples. The failures again occur through the Sn-rich regions in an intergranular fashion.

High and Low Temperature Thermal Cycling

In an effort to determine the effect of the high and low portion of the thermal cycle the following experiments were performed. The full -55°C to 125°C cycle was split into two equal cycles of -55°C to 35°C and 35°C to 125°C . The specimen length was increased to induce a 19% shear strain on cycling. A 10 mil (0.254 mm) 60Sn-40Pb solder joint thickness was used in these experiments.

• 35°C to 125°C

The 35°C to 125°C cycle shows the effect of the high temperature portion of the thermal cycle. Furthermore this thermal fluctuation is representative of the temperatures encountered in the power cycling of an electronic package.

The optical microstructure of the 60Sn-40Pb joints as a function of the number of cycles between 35°C and 125°C is shown in Figure 10. After 500 cycles the heterogeneous coarsened region develops in the center of the solder joint, in a fashion identical to that found for the full -55°C to 125°C thermal cycle.

Cracks develop in the coarsened regions after 1500 cycles. A higher magnification of these cracks is shown in Figure 11. The cracks preferentially occur through the Sn-rich phase or at the interphase boundaries. Cracking occurs in the Pb-rich phase only when a path through the Sn is not available. The similarities between the full thermal cycle and the high temperature cycle indicate that coarsening and cracking is dependant on strain at elevated temperatures.

- -55°C to 35°C.

Cycling between -55°C and 35°C examined the behavior of the solder joint at the low temperature portion of the thermal cycle. Figure 12 shows the optical microstructure of the joint as a function of cycles between -55°C and 35°C. Heterogeneous coarsening is not as extensive for this low temperature cycling. However, a very thin heterogeneously coarsened region in the solder does develop after 1500 cycles. This coarsening is shown clearly in Figure 13 for the sample after 1500 thermal cycles. A coarsened region develops both parallel to the shear direction and between columnar cells of the solder. Cracks develop in the thin coarsened regions, after 1500 cycles, and the cracks run through the Sn-rich regions or at interphase boundaries. Cracks were only observed within the coarsened regions.

Coarsening can occur at these low cycling temperatures because even at 35°C the solder is at 0.67 of its homologous temperature. With strain and temperature present at 35°C heterogeneous coarsening can occur but not to the same extent as at higher temperatures in the thermal cycle.

Thermal Cycling (-55 °C to 125 °C) of Unconstrained Bulk Solder

Unconstrained bulk 60Sn-40Pb solder was cycled between -55°C and 125°C to observe coarsening behavior as a function of temperature alone. Optical micrographs of the solder are shown in Figure 14 as a function of the number of cycles. Coarsening was observed to develop as the number of cycles increase. The coarsening was homogeneous in nature, both the Pb and Sn regions coarsened throughout the solder. The Sn grain size was found to be 1.3 μm from the TEM micrographs shown in Figure 8. The Pb-rich regions remain heavily decorated with Sn precipitates ranging from 0 cycles to 2000 cycles. In heterogeneous coarsening, described previously, the Pb-rich regions were denuded of precipitates. No cracking was observed to occur anywhere within the solder

for any number of cycles. The heterogeneous coarsening and cracking is therefore a function of temperature and applied strain.

Thermal Cycling of Cu/Solder/Cu Joints (-55 °C to 125 °C)

There exists a difference in the coefficients of thermal expansion between Cu (16.6 $\mu\text{in/in}^\circ\text{C}$) and 60Sn-40Pb solder (24.7 $\mu\text{in/in}^\circ\text{C}$). It has been suggested^{6,7} that failures of solder joints occur, in part, due to these differences. To study this possibility specimens of Cu/Solder/Cu joints were manufactured and thermally cycled from -55°C to 125°C. The only strain imposed in these specimens was due to the thermal expansion difference between the solder and the Cu.

Optical micrographs of the Cu/Solder/Cu joints as a function of the number of thermal cycles is shown in Figure 15. Heterogeneous coarsening does occur but only begins after 2000 cycles. The experiment ended after 2000 cycles and no cracks were observed anywhere within the joint. (The dark interfacial regions in the sample after 1000 cycles is a polishing artifact of the height difference between the solder and Cu.) It is expected that cracking would eventually occur in the coarsened region given enough thermal cycles. This indicates that the difference in expansion between solder and Cu is significant to the thermal fatigue failure of solder joints. However, this effect is not as prevalent as when an externally applied strain is present (i.e. when the joint is constrained between Cu and Al).

DISCUSSION

Heterogeneous coarsening was found to be the precursor to failure in 60Sn-40Pb joints at all temperature ranges tested in this work. Observations presented in the literature also show heterogeneous coarsening in solder joints in thermal fatigue. Wild⁵ has published optical micrographs of 60Sn-40Pb joints that show a coarsened region in the solder joint with a crack running through this region. However, no comment was made on the

phenomenon. Also Wild attributes the failure to slip across multiple Pb and Sn-rich phases. Multiple phase slip would be difficult as the phases are polygranular at a fine scale and contiguous slip planes are unlikely. Bangs and Beal¹² also observed coarsening but they do not attribute failures to the coarsened region. They claim failures to be due to interphase separation, and that the Sn-phase does not fail. Lynch et. al.²⁶ appreciated that coarsening is detrimental to fatigue life and did attribute failures as being due to the presence of coarsening of the solder. However, they performed no optical microscopy so their assumption was that the solder coarsens homogeneously due to aging at the high temperature side of the thermal cycle. Yenawine et. al.⁷ directly observed heterogeneous coarsening of the solder microstructure in electronic packages during thermal fatigue. They also state that the cracks run solely through the coarsened region. The coarsening in the Yenowine study was complicated as the solder joints do not experience simple shear deformation. However, the most extensive coarsening was found to occur in regions of the joint that encountered the highest shear strains.

Almost all observations in the literature of solder joint failures due to thermal fatigue state that the cracks run through the Pb-rich phase^{5,7,12,24}. Results of this current work, however, show that it is the Sn-rich phase that fails, Figure 10. The reason for this discrepancy could be that observations made in the literature were made well after final joint failure. The polishing of these joints could then cause the solder material adjacent to the crack to fall out. On subsequent observations it would then appear that the joint failed through the Pb-rich phase when the actual failure pattern was lost during polishing.

Heterogeneous coarsening was found in this study to occur in regions of high shear strain, at the ends of the specimen, more or less parallel to the direction of shear. The mechanism for the formation of a heterogeneous coarse band is not fully understood but a qualitative explanation is as follows. The shear strain across the solder joint is uniform in deformation but becomes concentrated due to some heterogeneity in the solder. Shear deformation in the joint then becomes localized at the heterogeneity inducing dislocations

and vacancies into the solder at this location. Upon thermal cycling the region adjacent to the heterogeneity undergoes phase growth. The dislocations and vacancies assist in diffusion causing this region to coarsen as the thermal cycling proceeds. The coarsened region is weaker than the rest of the solder in the joint²⁷ so subsequent deformation will further concentrate at the coarsened region. The initial heterogeneity is not necessarily associated with the interface between the solder and Cu as coarsening occurs both at the interface and in the center of the joint.

The cause of the initial heterogeneity appears to be associated with the boundaries between the eutectic Sn-Pb colonies within the solder joint. The boundary between the colonies consists of Sn and Pb-rich phases that are initially, on solidification, coarser than the rest of the microstructure. Therefore the boundaries are the weakest portion of the microstructure and the strain concentrates there. Further coarsening is also facilitated because the regions adjacent to the coarsening are fine and redistribution of Pb and Sn is easy, Figure 4.

The failure of 60Sn-40Pb joints was found to initiate in the Sn-rich phase, within the coarsened region. The cracks propagated intergranularly through the Sn-Sn grain boundaries. A possible mechanism for these failures is related to the mode of deformation utilized by near-eutectic Sn-Pb alloys. Fine grained near-eutectic Sn-Pb alloys are superplastic²⁸ and deform by grain rotation and grain boundary sliding. The initial microstructure of the 60Sn-40Pb joint consists of an interconnected Sn-rich phase. The initial Sn grain size was found to be 0.44 μm . The Sn grain size after thermal cycling in the heterogeneously coarsened region increases to about 3 μm . At this large grain size the Sn grains can no longer easily rotate and slide to accommodate the imposed strain, so intergranular cracks develop at the Sn-Sn grain boundaries. Once the interconnected Sn phase fails cracks form across the Pb-rich regions.

One suggestion for eliminating thermal fatigue failures in 60Sn-40Pb joints is to match the thermal expansion coefficients of the materials joined by the solder. Besides

being an expensive proposition, matching the materials only slightly delays failures. The optical micrographs in Figure 15 show that even the difference in thermal expansion between Cu and 60Sn-40Pb solder causes heterogeneous coarsening to occur. Eventually cracks will form in the coarsened region leading ultimately to failure.

Both high (35°C to 125°C) and low (-55°C to 35°C) temperature thermal cycles were detrimental to the fatigue life of 60Sn-40Pb solder joints. The high temperature cycling coarsened and failed in a manner identical to that for the full -55°C to 125°C cycle, Figure 10. This indicates that the coarsening and failure is temperature dependant and occurs at the high temperature portion of the thermal cycle. However, the solder does coarsen and fail even in low temperature cycling. For the low temperature cycling the high portion of the cycle, 35°C, is still 0.69 of the homologous temperature. Therefore even room temperature and below cycling results in high temperature deformation processes in 60Sn-40Pb solder.

All failures in this study were found to occur in the bulk solder of the joint. This indicates that interfacial intermetallics have little, if any, influence on the thermal fatigue behavior of 60Sn-40Pb solder joints. Some work has shown²⁹ that on isothermal shear to failure tests that 60Sn-40Pb joints do fail through interfacial intermetallics, but only at very rapid deformation rates. At slower deformation rates failures only occurred through the bulk of the solder. The thermal fatigue tests in this study induced strain rapidly via thermal shock (cold liquid bath to hot liquid bath) and interfacial failures were not observed. Therefore in actual use, where strains are induced more slowly, the solder joints of an electronic package should not fail through interfacial intermetallics.

SUMMARY AND CONCLUSIONS

Thermal fatigue tests were performed using a specimen designed to impose simple shear strain on solder joints in thermal cycling. 60Sn-40Pb joints were tested with a maximum shear strain of 19% imposed. The nominal thermal cycle was -55°C to 125°C.

The failures in 60Sn-40Pb joints were preceded by heterogeneous coarsening of the solder. Both the Pb and Sn-rich phases were found to coarsen. The Pb-rich phase was found to be denuded of precipitates. The heterogeneous coarsening was due to strain imposed in thermal cycling by the thermal expansion differences between joined materials. Only homogeneous coarsening was observed in unconstrained bulk solder specimens. Heterogeneous coarsening was also observed when the only strain imposed was due to the difference in thermal expansion between the solder and the joined material. This indicates that by designing a joint to have matched expansion coefficients only delays thermal fatigue failures, it does not eliminate them.

The heterogeneous coarsening arises at some heterogeneity in the solder that concentrates the shear strain at one point in the joint. The concentrated strain results in phase growth at the heterogeneity. The coarsened region is the weakest point of the joint leading to further coarsening on continued thermal cycling.

The 60Sn-40Pb joints crack through the heterogeneous coarsened regions. The cracks are intergranular through the interconnected Sn-rich phase at Sn-Sn grain boundaries. The Sn grains are large in the coarsened region so that they can no longer rotate and slide to accommodate the strain. This results in cracks at Sn grain boundaries. All failures were observed to occur only through the bulk solder of the joint.

Experiments were performed at low (-55°C to 35°C) and high (35°C to 125°C) thermal cycles. The elevated temperature portion of the cycle was found to be the source of coarsening and failure. The 35°C to 125°C cycled specimens failed in a fashion identical to the -55°C to 125°C cycle. The low temperature cycle also failed, after a larger number of cycles, through a thin heterogeneous coarsened region. Low temperature failures occurred because even at 35°C the solder is at 0.69 of the homologous temperature and there is enough thermal energy for coarsening to occur.

ACKNOWLEDGEMENTS

This work was supported by the Director, Office of Energy Research, Office of Basic Energy Science, Material Sciences Division of the U. S. Department of Energy under contract #DE-AC03-76SF00098.

REFERENCES

1. E. Levine and J. Ordenez; IEEE Trans. Components, Hybrids, and Manufacturing Tech. *CHMT-4* , 515 (1981) .
2. S. K. Kang, N. D. Zommer, D. L. Feucht, R. W. Heckel; IEEE Trans. Parts, Hybrids, and Packaging *PHP-13* , 318 (1977) .
3. J. T. Lynch, M. R. Ford, A. Boetti; IEEE Trans. Components, Hybrids, and Manufacturing Tech. *CHMT-6* , 237 (1983) .
4. J. W. Munford; IEEE Trans. Parts, Hybrids, and Packaging *PHP-11* , 296 (1975).
5. R. N. Wild; "Fatigue properties of solder joints", *Welding Research Supp.* 51 , 521s (1972).
6. E. A. Wright, W. M. Wolverton; "The effect of the solder reflow method and joint design on the thermal fatigue life of leadless chip carrier solder joints", *Proc. 34th Electron. Components Conf.*, *34* , 149 (1984) .
7. R. Yenawine, M. Wolverton, A. Burkett, B. Waller, B. Russel, D. Spritz; "Today and tomorrow in soldering", *Proc. 11th Naval Weapons Electronics Manufacturing Seminar, China Lake, CA* (1987) p. 339.
8. H. B. Ellis; "Aspects of surface mounted chip carrier solder joint reliability", *Proc. 11th Naval Weapons Electronics Manufacturing Seminar, China Lake, CA* (1987) p. 377.
9. D. R. Olsen, A. M. Berg; IEEE Trans. Components, Hybrids, and Manufacturing Tech. *CHMT-2* , 257 (1979).

10. L. S. Goldmann, R. D. Herdzik, N. G. Koopman, V. C. Marcotte; IEEE Trans. Parts, Hybrids, and Packaging *PHP-13* , 194 (1977).
11. H. S. Rathore, R. C. Yih, A. R. Edenfeld; J. Testing and Evaluation *1* , 170 (1973).
12. E. R. Bangs, R. E. Beal; Welding Res. Supp. *54* , 377s (1975) .
13. K. C. Norris, A. H. Landzberg; IBM J. Res. Dev. *13* , 266 (1969).
14. G. Becker; "Testing and results related to the mechanical strength os solder joints", IPC Fall meeting IPC-TP-288 (1979) .
15. E. C. Kubik and T. P. L. Li; "Thermal shock and temperature cycling effects on solder joints of hermetic chip carriers mounted on thick films", Microelectronics Center, Martin Marrietta Aerospace, Orlando FL 32855.
16. P. M. Hall, T. D. Dudderar, J. F. Argyle; IEEE Trans. Components, Hybrids, and Manufacturing Tech. *CHMT-6* , 544 (1983).
17. D. Frear, D. Grivas, M. McCormack, D. Tribula, J. W. Morris, Jr.; "Fatigue and thermal fatigue of Pb-Sn solder joints", Proc. Effects of Load and Thermal Histories on Mechanical Behavior Symp. AIME Spring Conf., Denver, CO (1987) ,in press.
18. D. Frear, D. Grivas, M. McCormack, D. Tribula, J. W. Morris, Jr.; "Fatigue and thermal fatigue testing of Pb-Sn solder joints", Proc. 3rd Ann. Electronic Packaging and Corrosion in Miroelectronics Conf., *3* , 269 (1987).
19. H. N. Keller; IEEE Trans. Components, Hybrids, and Manufacturing Tech. *CHMT-4*, 132 (1981).
20. P. M. Hall; IEEE Trans. Components, Hybrids, and Manufacturing Tech. *CHMT-4*, 403 (1981).
21. K. R. Stone, R. Duckett, S. Muckett, M. E. Warwick; Brazing and Soldering *4* , 20 (1983).
22. C. Wright; IEEE Trans. Parts, Hybrids, and Packaging, *PHP-13* , 202 (1977).
23. M. C. Denlinger, D. W. Becker; Welding Res. Supp. *57* , 292s (1978).

24. R. N. Wild; "Some fatigue properties of solders and solder joints", IBM Report no. 74Z000481, Oct. (1975).
25. J. T. Lynch, G. M. Dydon, M. R. Hephher, J. P. McCarthy; "Environmental assesment of ceramic chip carriers soldered-attached to thick film alumina substrates", Proc. 32nd Elec. Comp. Conf., 32, 385 (1982).
26. W. T. Chen, C. W. Nelson; IBM J. Res. Dev. 23, 179 (1979).
27. C. J. Thwaites, W. B. Hampshire; Welding Res. Supp., 55 323s (1976).
28. D. Grivas; Deformation of Superplastic Alloys at Relatively Low Strain Rates, Ph.D. thesis, University of California, Berkeley (1978).
29. D. Frear, D. Grivas, L. Quan, J. W. Morris, Jr.; "Microstructural observations and mechanical behavior of Pb-Sn solder on Cu plates", Mat. Res. Soc. Symp., 72, 181 (1986).

FIGURE CAPTIONS

Fig. 1 Specimen used to test solder joints in thermal fatigue conditions.

Fig. 2 Digitally controlled crane used to cycle specimens between thermal baths.

Fig 3 Optical microstructure cross sections of 60Sn-40Pb/Cu joints as a function of the number of cycles between -55° and 125°C.

Fig. 4 Optical microstructure cross section of a 60Sn-40Pb/Cu joint after 684 cycles between -55° and 125°C revealing the heterogeneous coarsened region.

Fig. 5 Optical microstructure cross section of a 60Sn-40Pb/Cu joint after 1300 cycles between -55° and 125°C showing a crack in the coarsened region.

Fig. 6 Polarized optical microstructure cross section of a 60Sn-40Pb/Cu joint after 1300 cycles. Intergranular cracks through the Sn rich phase are shown.

Fig. 7 TEM bright field image of polygranular β -Sn in lamellar and globular regions in 60Sn-40Pb.

Fig. 8 TEM bright field image of polygranular β -Sn after 167 hours at 125°C illustrating Sn grain growth.

Fig. 9 Optical microstructure cross section of a 20 mil (0.51 mm) thick 60Sn-40Pb/Cu joint as a function of the number of thermal cycles between -55° and 125°C.

Fig 10 Optical microstructure cross sections of 60Sn-40Pb/Cu joints as a function of the number of cycles between 35° and 125°C.

Fig 11 Optical microstructure cross sections of 60Sn-40Pb/Cu joints after 1500 and 2000 cycles between 35° and 125°C revealing cracks through the coarsened regions.

Fig. 12 Optical microstructure cross sections of 60Sn-40Pb/Cu joints as a function of the number of cycles between -55° and 35°C.

Fig. 13 Optical microstructure cross section of a 60Sn-40Pb/Cu joint after 1500 cycles between -55°C and 35°C revealing a thin coarsened region and cracks propagating through the Sn-rich phase in this region.

Fig. 14 Optical microstructure of unconstrained 60Sn-40Pb bulk solder as a function of the number of cycles between -55° and 125°C.

Fig. 15 Optical microstructure cross sections of Cu/60Sn-40Pb/Cu specimens as a function of the number of cycles between -55° and 125° C. Heterogeneous coarsening is found at 2000 thermal cycles.

Thermal Fatigue Specimen

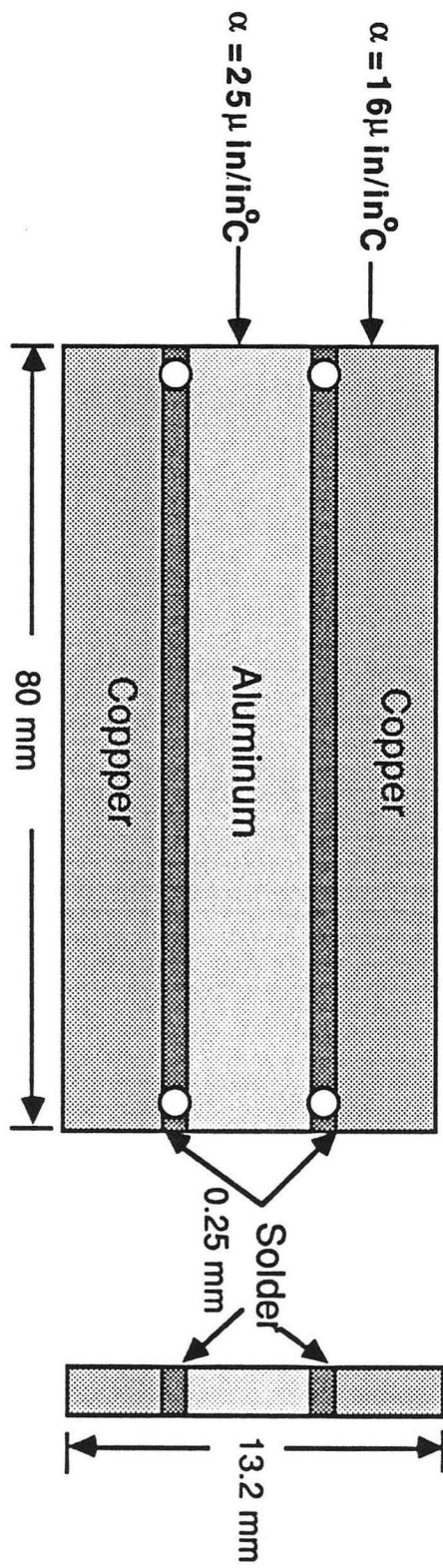
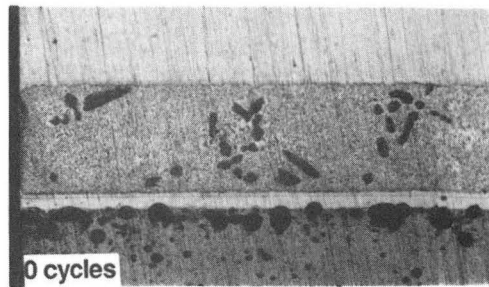


Fig. 1

60Sn-40Pb
Thermal Cycle: -55°C ↔ 125°C



- ← Cu
- ← Solder
- ← Cu/Ni Plate
- ← Al

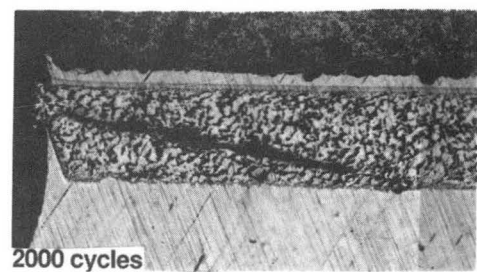
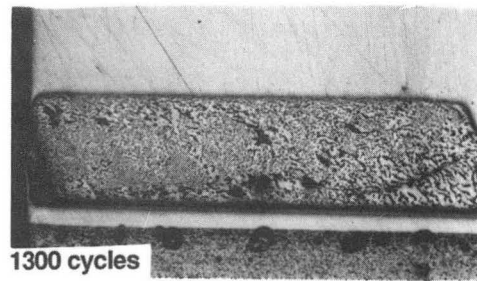
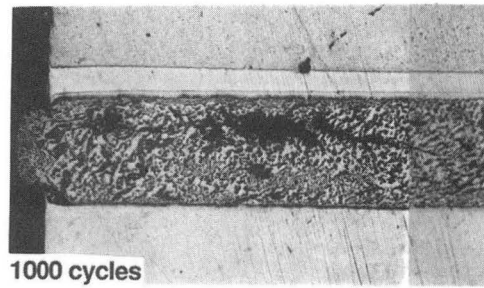
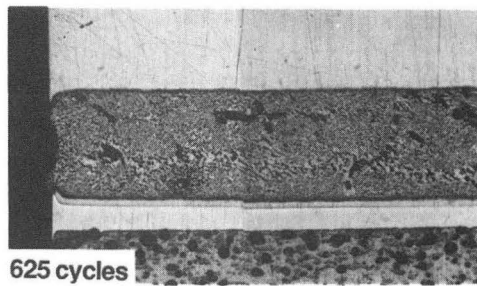
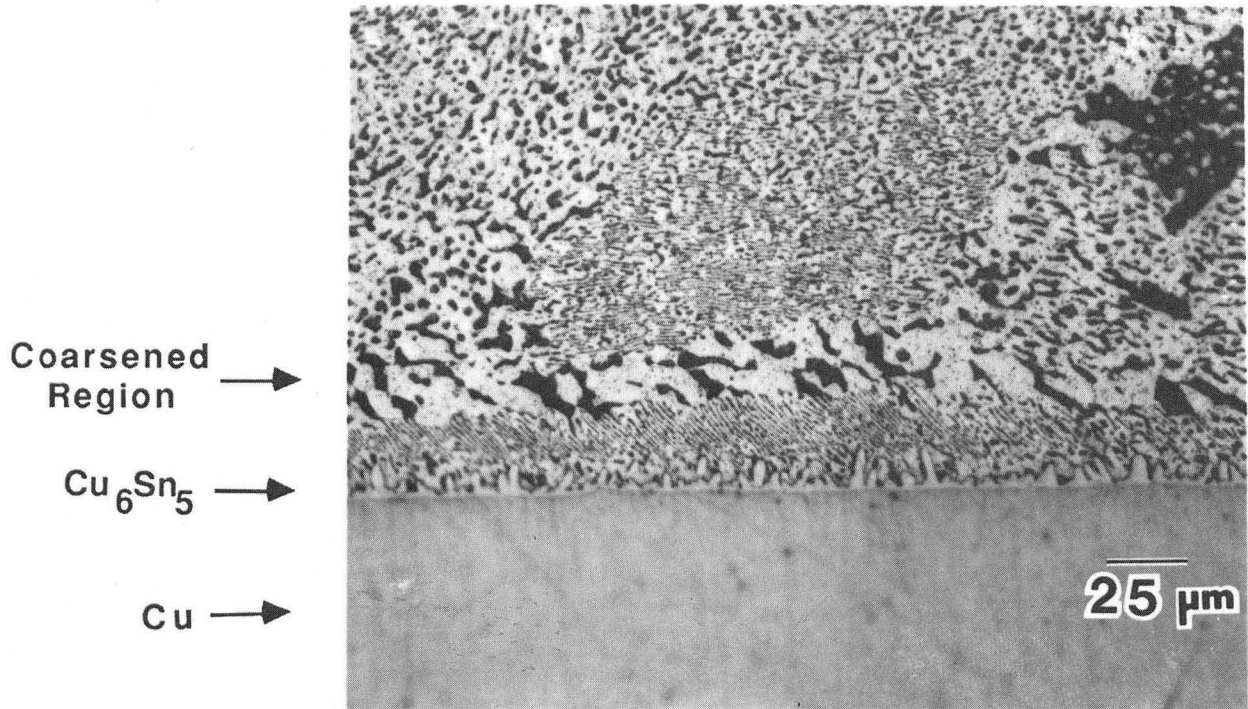


Fig. 3

XBB872-1250-A

1 mm



XBB870-10193

Fig. 4

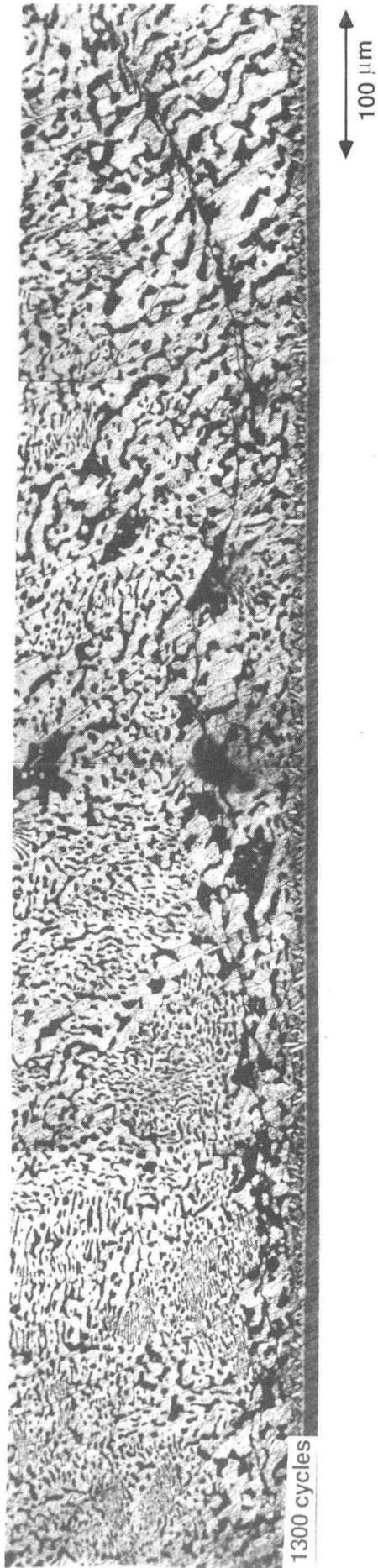


Fig. 5

Solder →
 Cu_6Sn_5 →
Cu →

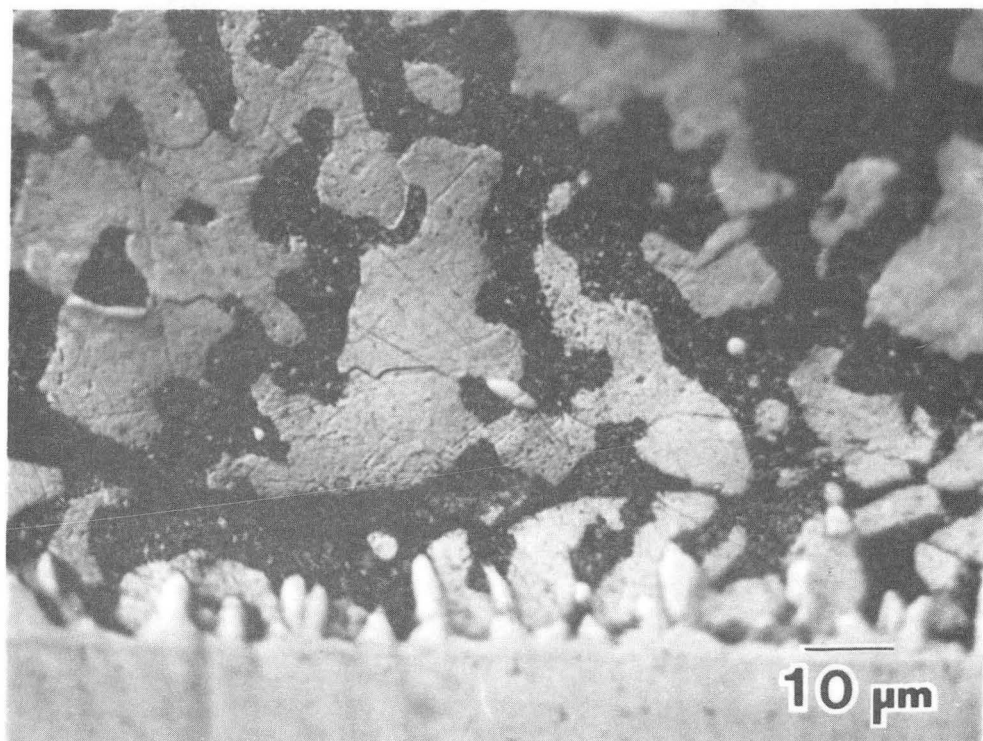
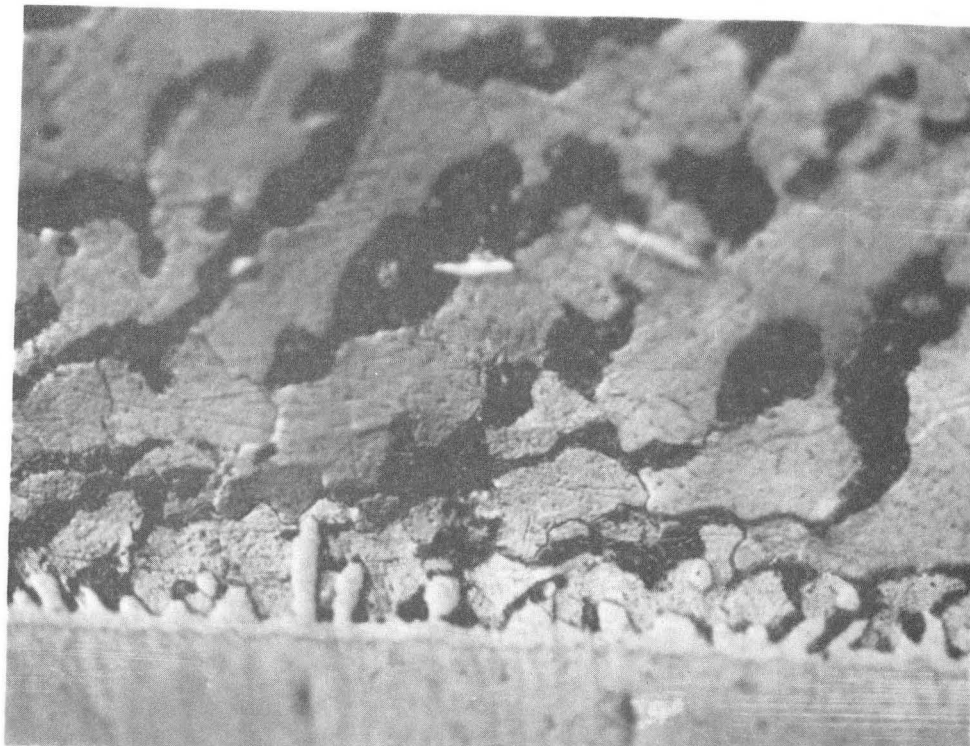
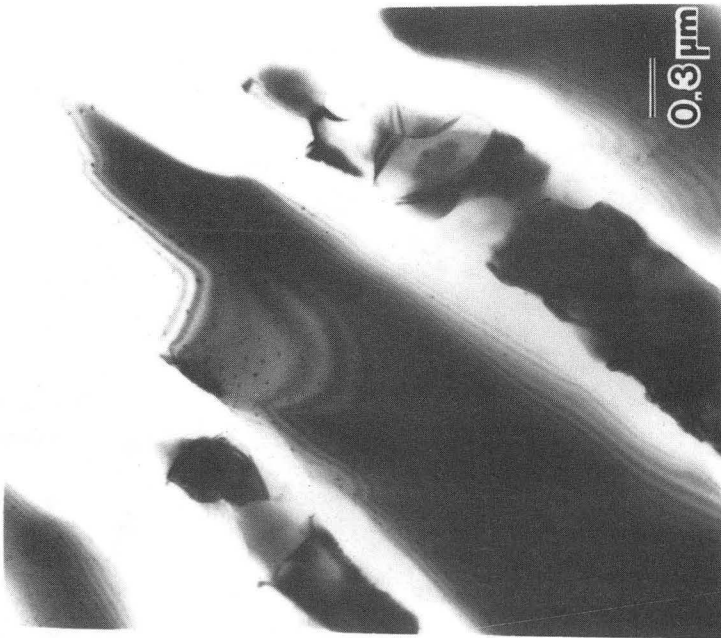
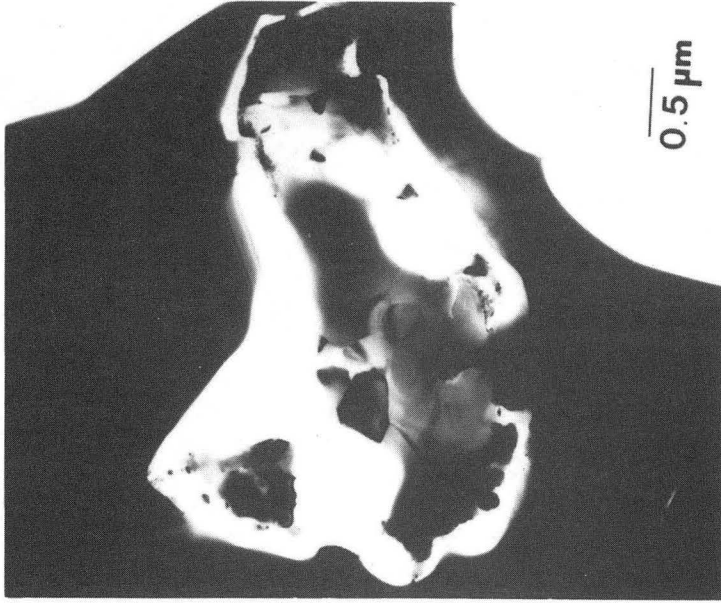


Fig. 6

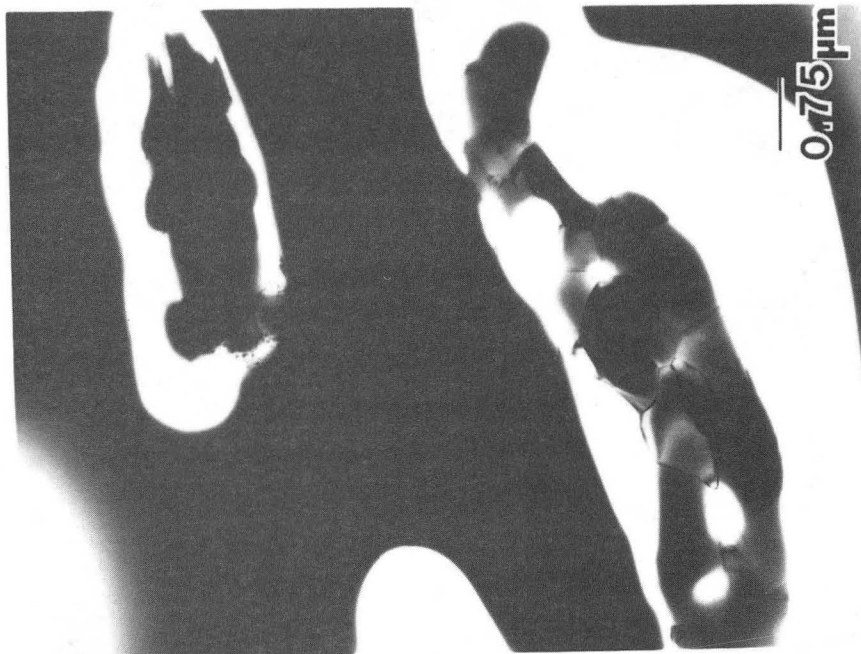


XBB860-10345-A

Fig. 7

α - Pb →

β - Sn ↗



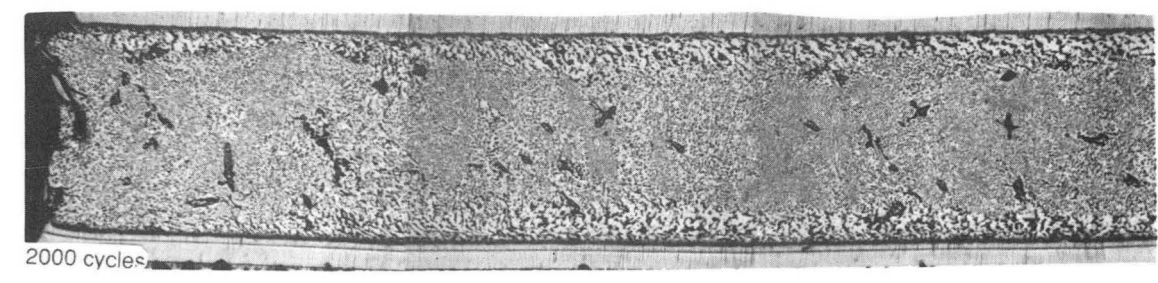
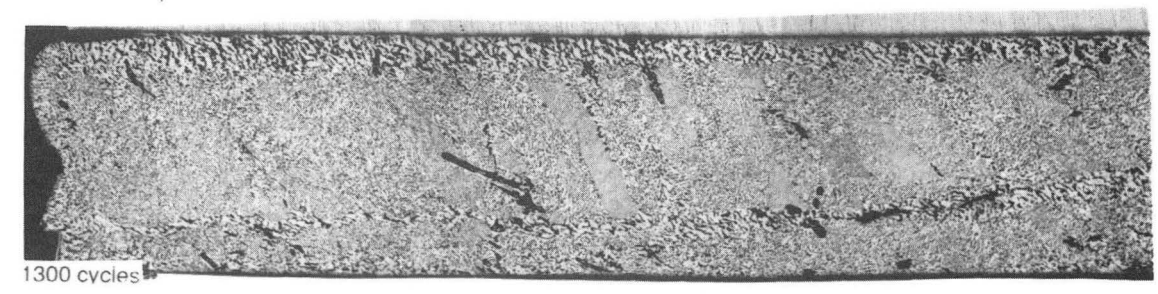
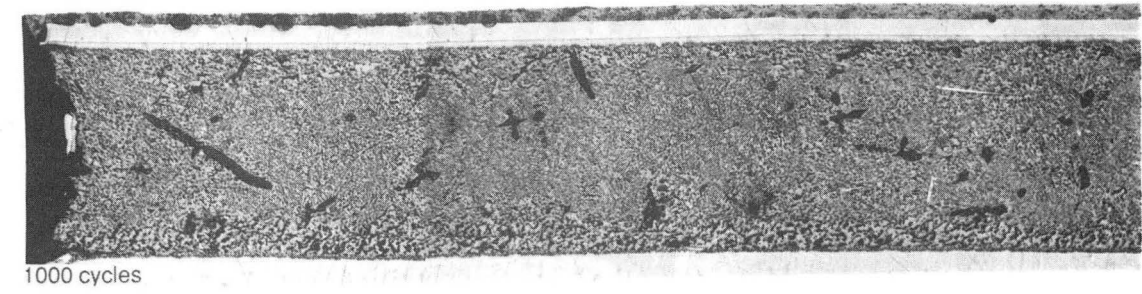
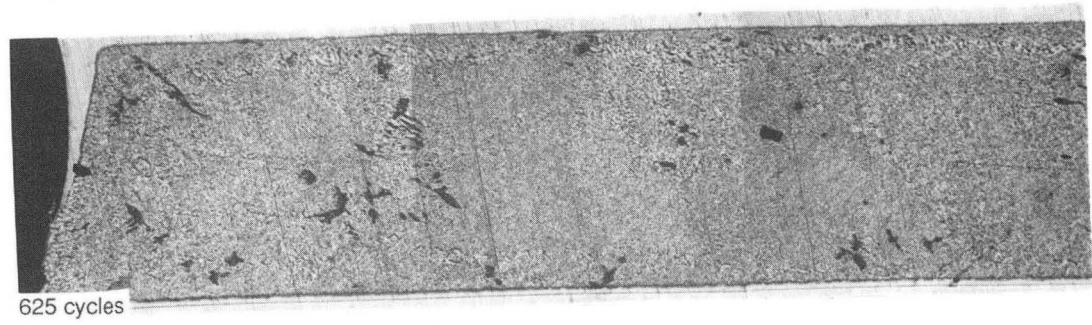
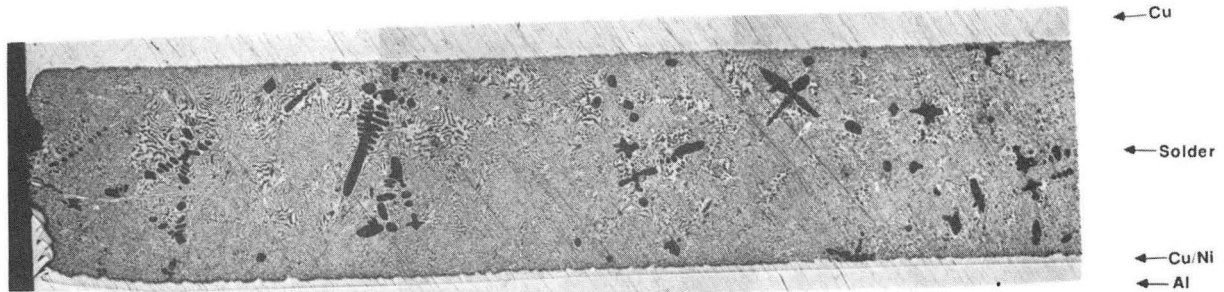
XBB875-3839-A

α - Pb →

β - Sn ↗

Fig. 8

60Sn-40Pb
Thermal Cycle: -55 C ↔ 125 C

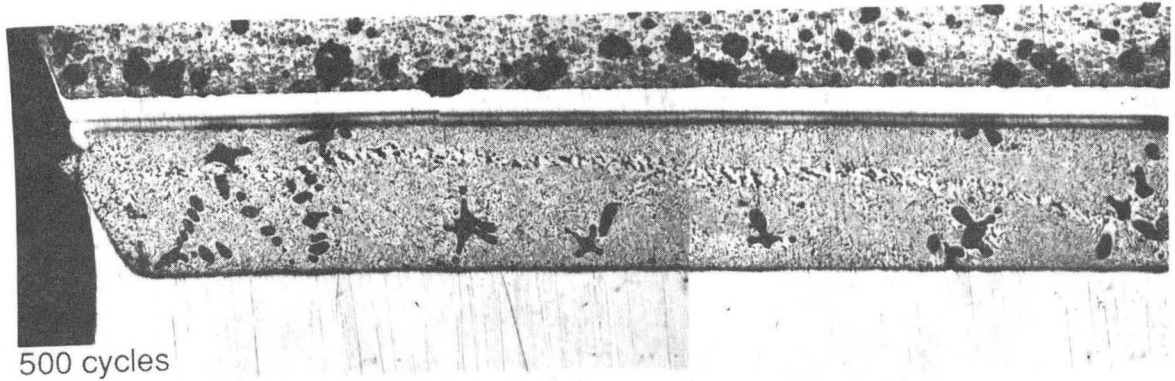


XBB874-3224-A

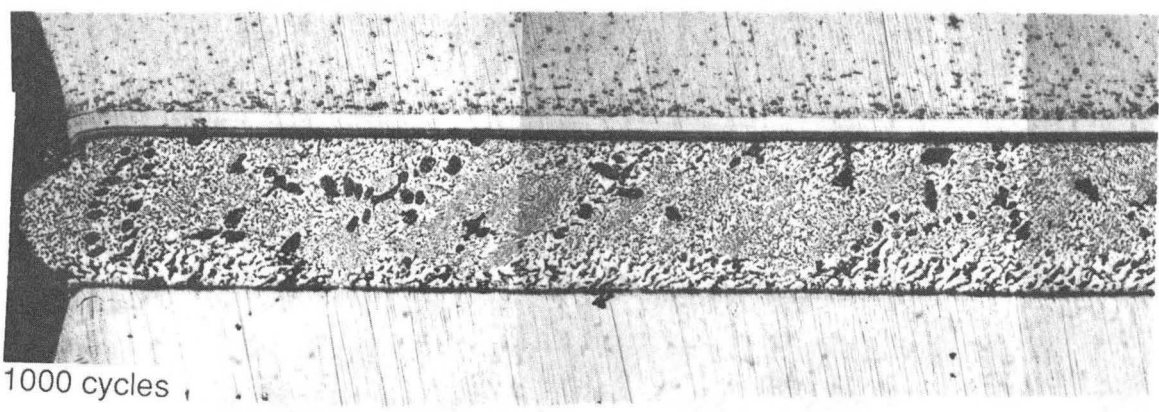


Fig. 9

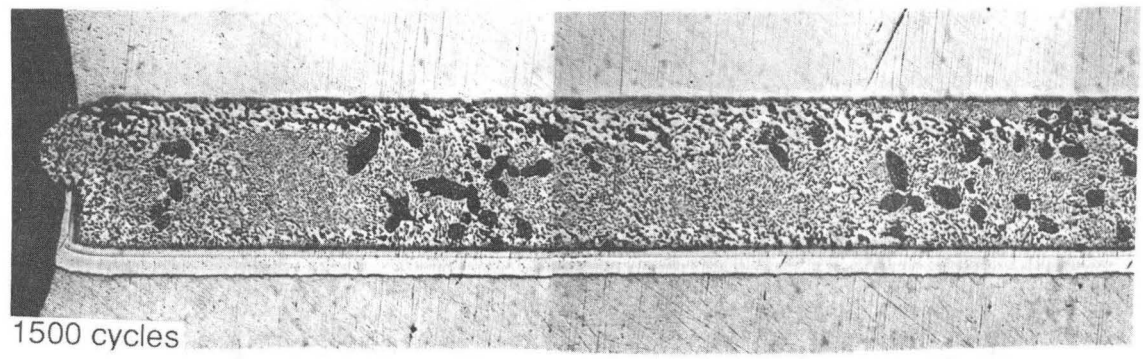
60Sn-40Pb
Thermal Cycle: 35°C ↔ 125°C



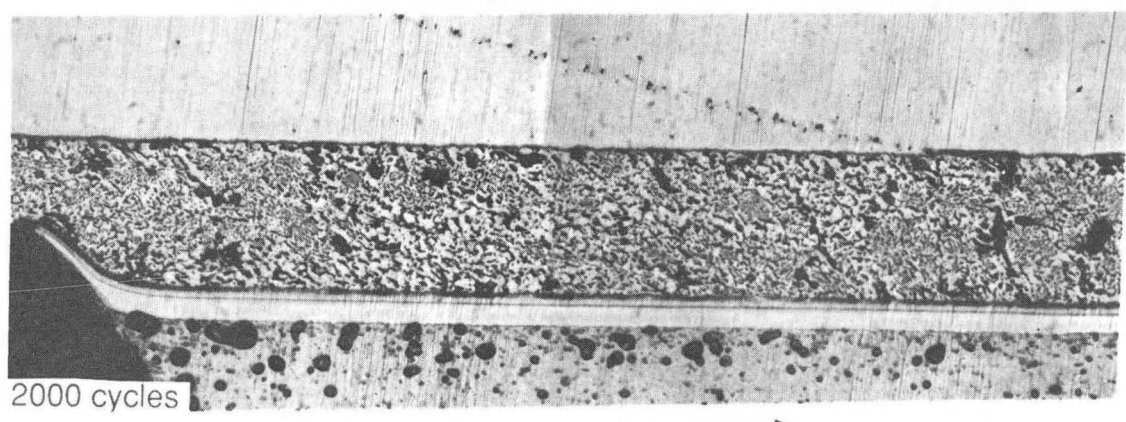
500 cycles



1000 cycles



1500 cycles



2000 cycles

XBB872-1253

← 1 mm →

Fig. 10

60Sn-40Pb
Thermal Cycle: 35°C ↔ 125°C

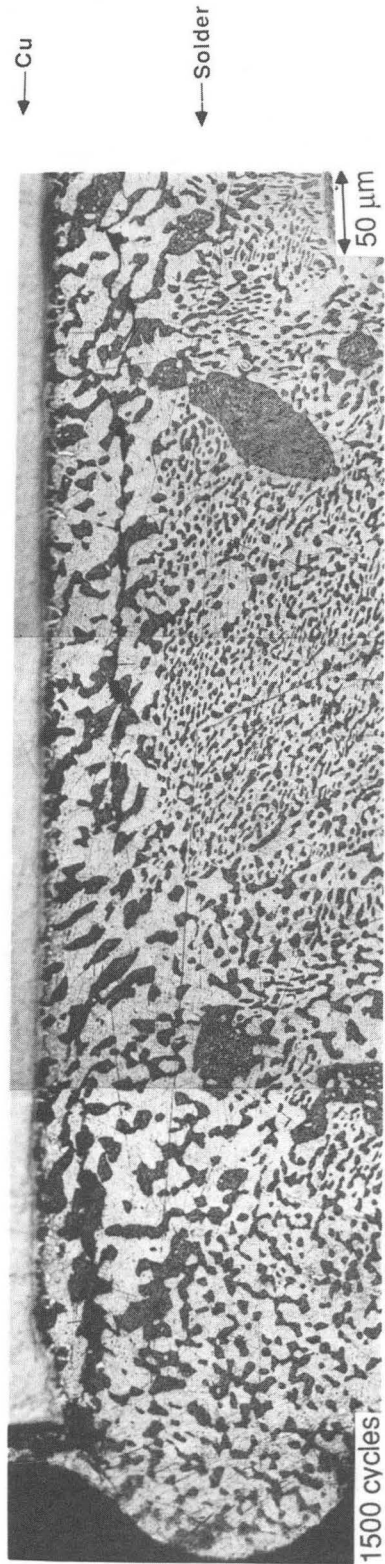
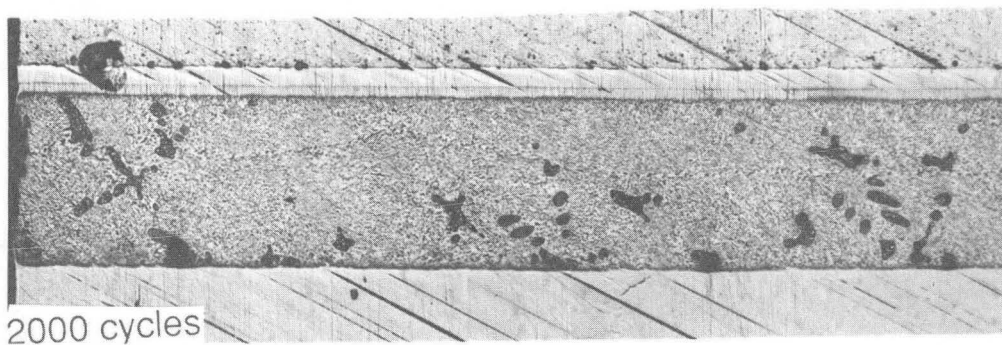
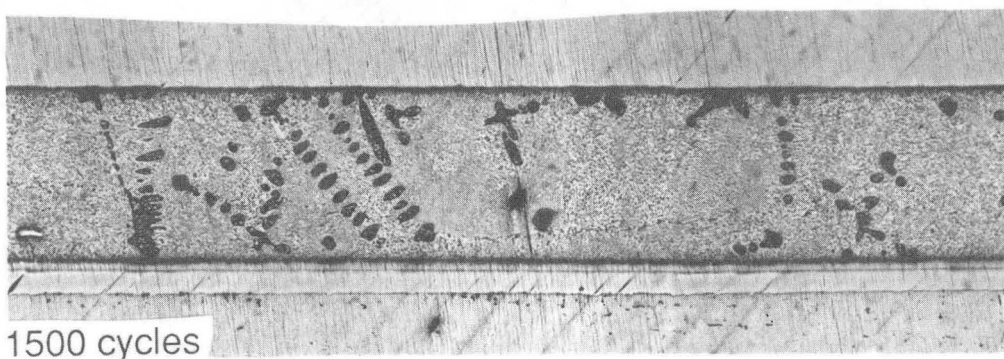
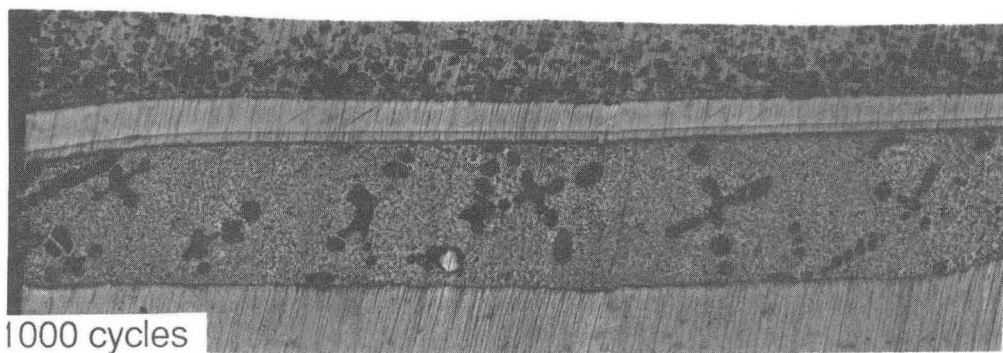
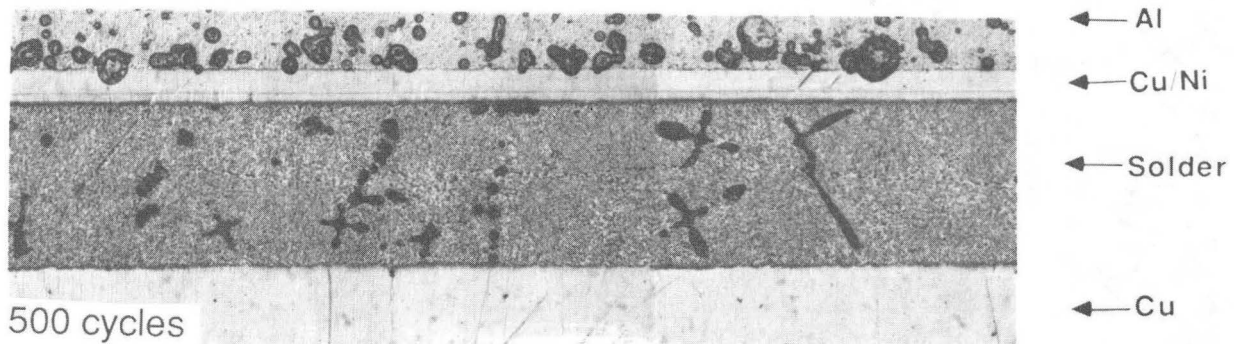


Fig. 11

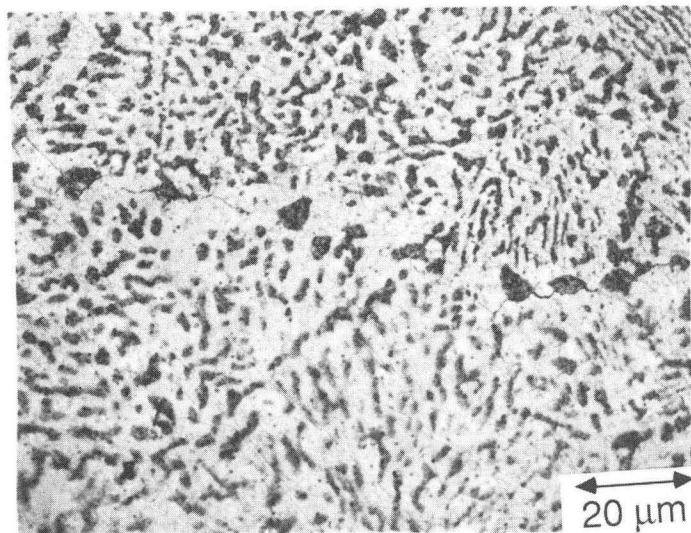
60Sn-40Pb
Thermal Cycle: $-55^{\circ}\text{C} \leftrightarrow 35^{\circ}\text{C}$



XBB872-1252-A

1 mm

Fig. 12



60 Sn-40Pb
Thermal Cycle: -55°C ↔ 35°C

1500 cycles

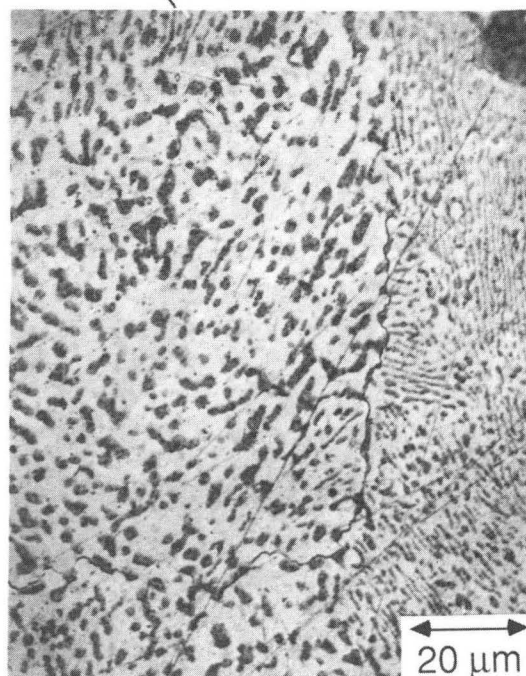
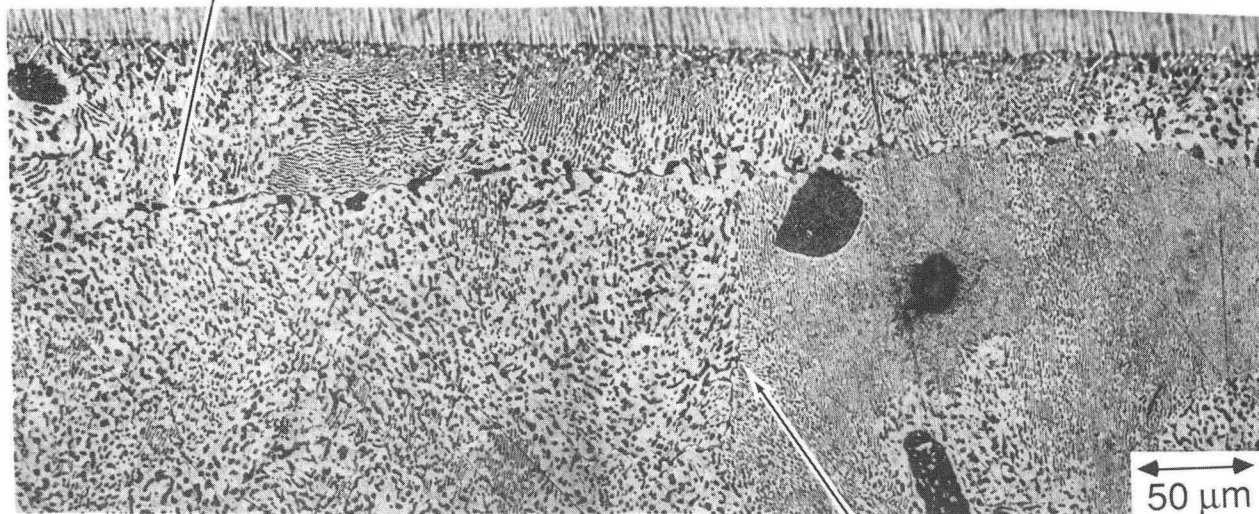
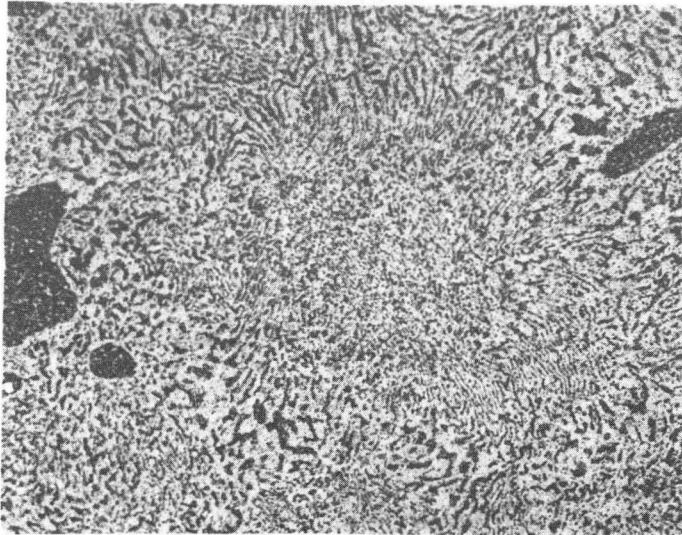


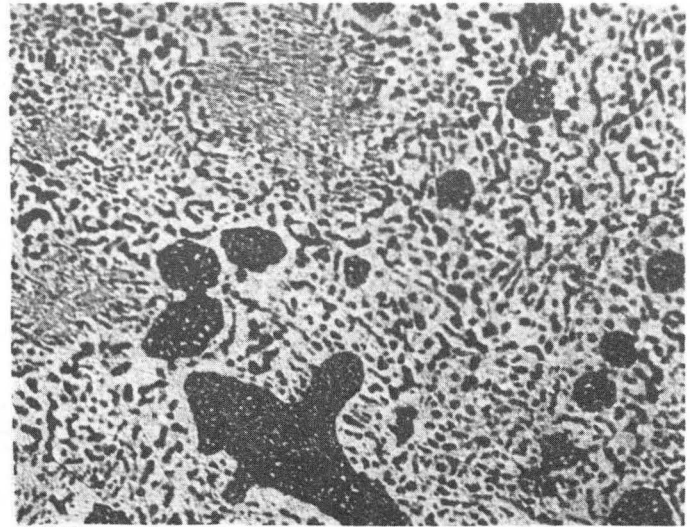
Fig. 13

Bulk 60Sn-40Pb Solder
Thermal Cycle: -55°C \longleftrightarrow 125°C

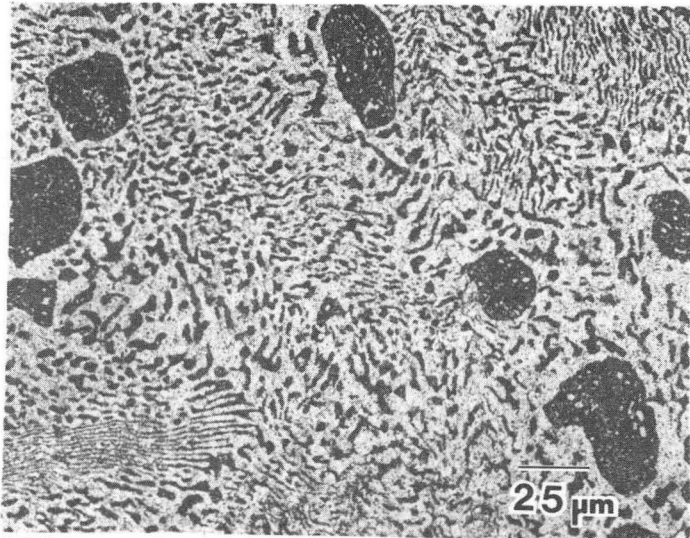
XBB872-1249



0 cycles

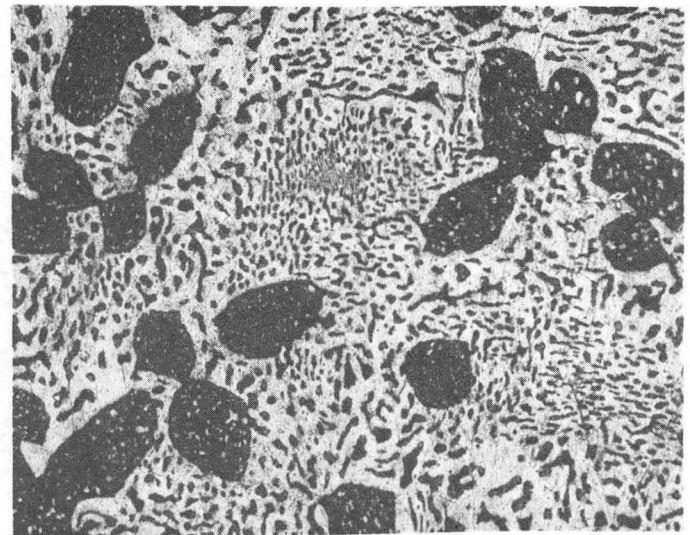


625 cycles



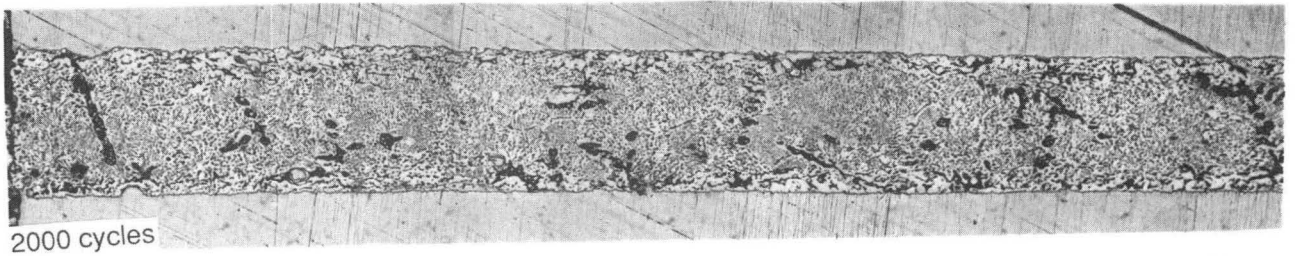
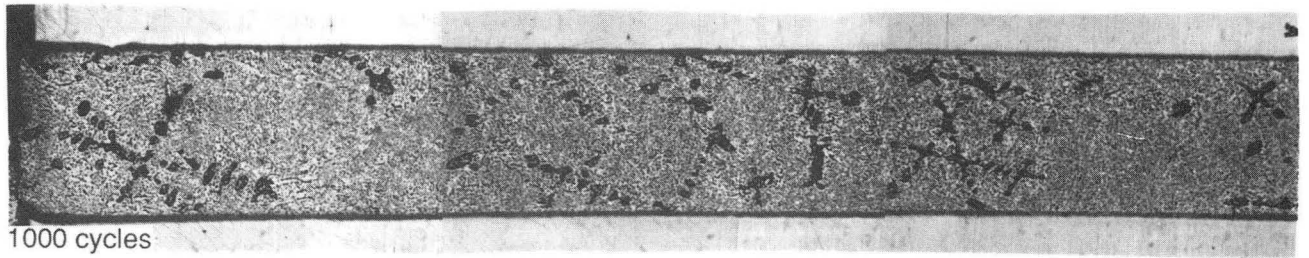
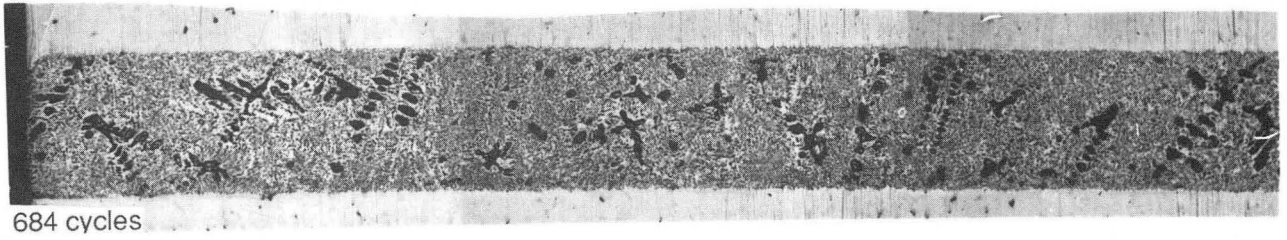
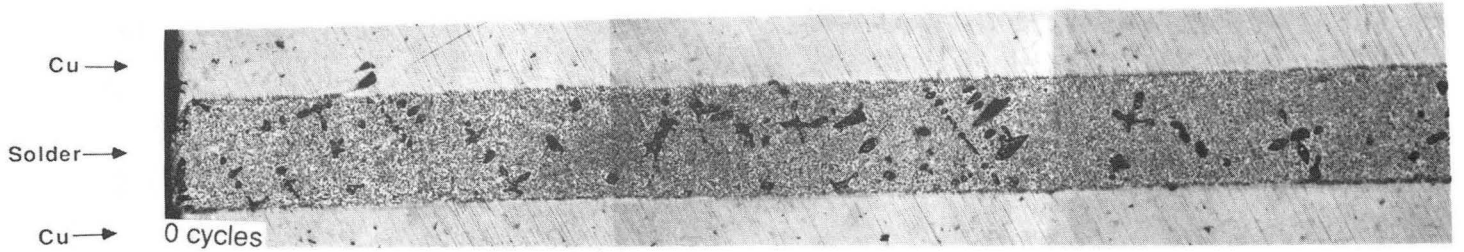
1000 cycles

Fig. 14



2000 cycles

60 Sn-40Pb
Thermal Cycle: -55°C ↔ 125°C
No Strain



XBB872-1251-A

↔
1 mm

Fig. 15

*LAWRENCE BERKELEY LABORATORY
TECHNICAL INFORMATION DEPARTMENT
UNIVERSITY OF CALIFORNIA
BERKELEY, CALIFORNIA 94720*